

Electronic Supplementary Information: Aqueous Citrate: a First-Principles and Force-field Molecular Dynamics Study.

Louise B. Wright^a, P. Mark Rodger^a and Tiffany R. Walsh^{b*}

a) Dept. of Chemistry and Centre for Scientific Computing, University of Warwick,
Coventry, CV4 7AL, U.K.

b) Institute for Frontier Materials, Deakin University, Geelong, 3216 Vic., Australia.

Contents

Figure E1: Typical example of an unphysical 1-5 intra-molecular hydrogen-bond formed using the GROMOS FF for citrate.

Finite-Size Effects: Details of system composition and computational set up used in Force-field MD simulations carried out in simulation cells of different dimensions.

Figure E2: HOCC and CCCC dihedral angles sampled by citrate in FF-s simulations of three different cell dimensions, initiated in starting configurations A and B. Data from the corresponding CPMD simulations is also presented for reference.

Figure E3: The three different possible conformations of the citrate ‘backbone’ considered in this study.

Non-bonded Force-field Parameters: Functional form of electrostatic and dispersion interactions in the citrate force-field.

Figure E4: The CHARMM atom-type assigned to each atom in citrate.

Table E1: Non-bonded parameters for citrate, taken from existing parameters in the CHARMM FF.

Bonded Parameters: Summary of the functional forms for the bonded interactions in the citrate force-field.

Table E2: Bonded parameters for V^{bond} .

Table E3: Bonded parameters for V^{angle} .

*tiffany.walsh@deakin.edu.au

Table E4: Bonded parameters for $V^{dihedral}$.

Table E5: Bonded parameters for $V^{improper}$.

Figure E5: Optimal geometry of the citrate anion *in vacuo* in a number of different internal configurations identified by calculations at the MP2/6-31G* level.

Figure E6: Potential energy scans of HOCC dihedral for each of the optimised structures of citrate *in vacuo* shown in Figure E5.

Table E6: Average number and average length of citrate···water hydrogen-bonds found in CPMD and FF-s simulations initiated in configurations A, B and C.

Figure E7: RDF profiles for citrate a) carboxylate– and b) hydroxyl– O_w and H_w distances for FF-s and FF-l simulations initiated in C conformation.

Hydrogen-Bond Strength Discussion of the strength of citrate···water hydrogen-bonding as defined by Furmanchuk *et al.*¹ or Lee *et al.*²

Figure E8: Hydrogen-bond strength (defined by the ratio g^{max}/g^{min}) for OM-water, OE-water and OH-water hydrogen-bonds; a comparison between CPMD, FF-s and FF-l simulations.

Figure E9: Hydrogen-bond strength (defined as being proportional to $1/r_{O-H}^4$) for OM-water, OE-water and OH-water hydrogen-bonds; a comparison between CPMD, FF-s and FF-l simulations.

Table E7: Continuous hydrogen-bond lifetimes, τ_s , for citrate-water and internal citrate hydrogen-bonds found in both CPMD and FF-s simulations.

Figure E10: Continuous hydrogen-bond time-autocorrelation functions, $S(t)$, for carboxylate···water hydrogen-bonds.

Amino Acid Simulation Methods: Details of the glycine and, serine and threonine simulations using CHARMM carried out to probe the persistence of water–carboxylate and water–hydroxyl interactions, respectively.

Figure E11: Intermittent hydrogen-bond time-autocorrelation functions ($C(t)$) for carboxylate···water hydrogen-bonds.

Table E8: Percentage probability of citrate possessing an internal hydrogen-bond and the probability of it adopting a folded (F), partially folded (P) or extended (E) carbon backbone conformation in the extended force-field simulations carried out under aqueous conditions.

Table E9: Percentage probability of a structure being internally hydrogen-bonded for each carbon backbone conformation–folded (F), partially folded (P) or extended (E).

Table E10: Percentage probability of citrate, when featuring an internal hydrogen-bond, to be co-ordinated by n Na^+ ions.

Figure E12: Percentage probability of an Na^+ ion being co-ordinated to 1, 2 or 3 oxygen atoms in citrate for each type of citrate- Na_n^+ ion pair.

Table E11: Summary of the three most populated co-ordination states of Na^+ ions surrounding citrate.

Citrate Input Files: Contents of two key input files in GROMACS format: **a)** structure file (citrate.gro), and **b)** topology file (citrate.top).

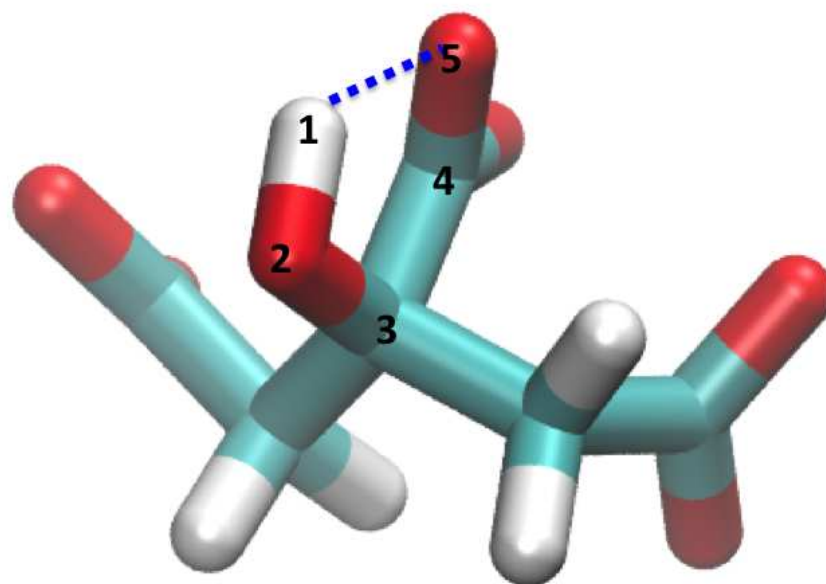


Figure E1: Example snapshot of the 1-5 internal hydrogen-bond formed by citrate, when using either the GROMOS or additive CHARMM parameters only. Carbon atoms are green, oxygen red and hydrogen white. The hydrogen-bond is represented by a dashed blue line.

Finite-Size Effects

The extreme computational expense of first-principles simulations, relative to force-field-based simulations, limits the physical size of a system that can be studied. While the CPMD simulations performed in this work were of comparable dimension to other recent studies,^{1,3–5} it was necessary to check that any potential system-size dependent artifacts, due to the periodicity imposed on the system under these conditions, were not incorporated into the force-field (FF) during our parametrisation process. Although the very nature of the issue cannot at present be probed directly by use of CPMD simulations of larger dimension to verify this, we can however check that the results from the FF simulations are invariant to changes in system size. Therefore four additional FF-s simulations were performed; two initiated in starting configuration A, and, two in starting configuration B. In one set of simulations, denoted ‘small’, a cell of dimensions comparable to CPMD was used. We point out here that interpretation of results generated with such a small system size for FF-based simulations inevitably comes with its own caveats, specifically due to the very short interaction cutoffs that are required (*vide infra*). In another set of runs, denoted ‘Large’, simulations were carried out in a simulation cell of ~ 40 Å in length. The parameters used to model the citrate anion in both sets of calculations were those derived from simulations in which a cell of dimension ~ 30 Å was used—see ‘Methods: Force-field MD Simulations’ in the main text for details.

Specifically, ‘small’/‘large’ simulations comprised one citrate, 3 Na⁺ and 128/2187 TIP3P water molecules respectively. In the case of the ‘small’ run, simulations were carried out in the *NVT* ensemble; non-bonded electrostatic summation was cut-off at 7 Å with a force-switching potential applied at 6.5 Å. Lennard-Jones interactions were cut-off at 7 Å with a switching potential applied at 6 Å. We remark that these cut-offs are much smaller than those recommended for the CHARMM FF, and emphasise that these small cut-offs are a consequence of the size of the simulation cell, recognising that the findings from these runs have caveats of their own. The ensemble and cut-offs used in the ‘large’ simulations were identical to those adopted for those performed for our conventional cell of dimension ~ 30 Å as reported in the main text. All other simulation details (for example time-step, integration algorithm) were identical to FF-s simulations carried out in a cell of dimension 30 Å see

‘Methods: Force-field MD Simulations’ in the main text.

The results of FF-s ‘small’ and ‘large’ simulations are presented in Figure E2. The conformations of the citrate anion, as probed by the HOCC and CCCC dihedral angles sampled during the course of these trajectories demonstrate invariance to system size.

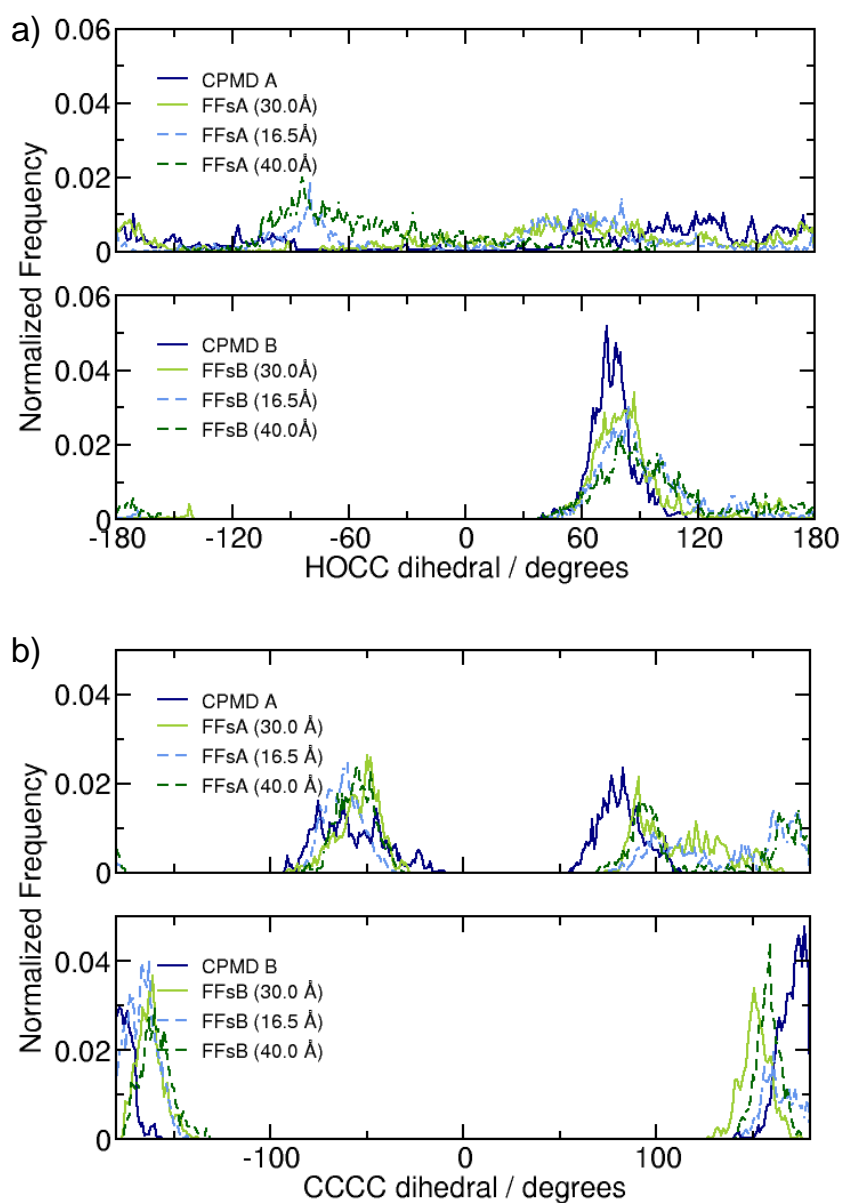


Figure E2: a) HOCC and b) CCCC dihedral angles sampled by citrate in FF-s simulations of three different cell dimensions (16.5 Å ‘small’, 30.0 Å and 40.0 Å ‘large’), initiated in starting configurations A and B. Data from the corresponding CPMD simulations are also presented for reference.

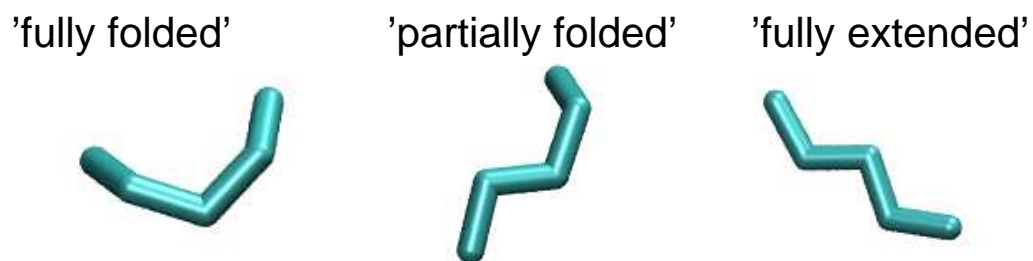


Figure E3: Three different possible conformations of the 'backbone' (chain of 5 consecutive C atoms from one terminal carboxylate group to the other) of a citrate molecule referred to in this paper: 'fully folded', 'partially folded' and 'fully extended'.

Non-bonded parameters

Non-bonded interactions in the new citrate FF are described by the following potential:

$$V^{NB}(r_{ij}) = 4\varepsilon_{ij} \left(\left(\frac{\sigma_{ij}}{r_{ij}} \right)^{12} - \left(\frac{\sigma_{ij}}{r_{ij}} \right)^6 \right) + C \frac{q_i q_j}{r_{ij}} \quad (1)$$

where $C = \frac{1}{4\pi\varepsilon_0\varepsilon_r}$; r_{ij} is the distance between atoms i and j ; σ_{ij} and ε_{ij} the van der Waals diameter and the strength of the interaction, respectively, between of atoms i and j ; q_i the partial charge of atom i ; and, ε_r the relative dielectric constant of the medium. The Lorentz-Berthelot mixing rules, $\sigma_{ij} = (\sigma_i + \sigma_j)/2$, $\varepsilon_{ij} = \sqrt{\varepsilon_i \times \varepsilon_j}$, are used to combine Lennard Jones parameters from different atom-types.⁶ In accordance with CHARMM, non-bonded interactions between atoms separated by 2 bonds or less are excluded, whilst as discussed in Section 'Force-Field Derivation' in the main text, the 1-5 electrostatic interaction between the citrate hydroxyl hydrogen and OM oxygen was scaled by a factor of 0.3.

Parameters for citrate, q_i , σ_i and ε_i , are listed in Table E1. Atom-types correspond to the specific atoms labeled in Figure E3.

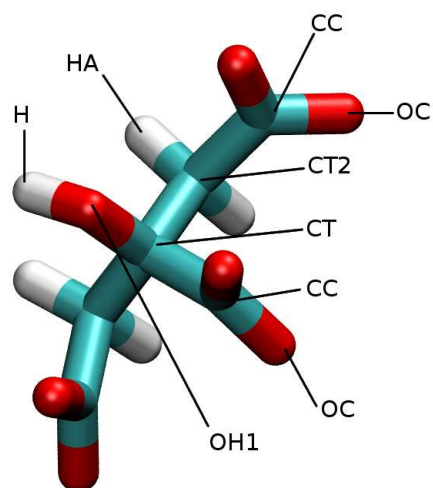


Figure E4: CHARMM atom-type assigned to each atom in citrate.

Atom-Type	q	σ (/ Å)	ϵ (/kJ mol ⁻¹)
OC	-0.760	3.02906	0.50208
CC	+0.620	3.56359	0.29288
HA	+0.090	2.35197	0.09205
CT2	-0.180	3.87541	0.23012
CT	-0.070	4.05359	0.08368
OH1	-0.540	3.15378	0.63639
H	+0.310	0.40001	0.19246
NA+	+1.000	2.42993	0.19623

Table E1: Non-bonded parameters for citrate (and Na⁺), taken from existing parameters in the CHARMM FF.

Bonded Parameters

Bonded interactions between citrate atoms are described by the following potential:

$$V^B = V^{bond} + V^{angle} + V^{dihedral} + V^{improper} \quad (2)$$

where:

$$V^{bond}(b_{ij}) = \frac{1}{2}k_{ij}^b(r_{ij} - b_{ij})^2 \quad (3)$$

$$V^{angle}(\theta_{ijk}) = \frac{1}{2}\theta_{ijk}^0(\theta_{ijk} - \theta_{ijk}^0)^2 + \frac{1}{2}k_{ijk}^{UB}(r_{ik} - r_{ik}^0)^2 \quad (4)$$

$$V^{dihedral}(\phi_{ijkl}) = k_{ijkl}^\phi(1 + \cos(n\phi_{ijkl} - \phi_{ijkl}^0)) \quad (5)$$

$$V^{improper}(\eta_{ijkl}) = \frac{1}{2}k_\eta(\eta_{ijkl} - \eta_0)^2 \quad (6)$$

		$b_0/\text{\AA}$	$k_b/\text{kJ mol}^{-1}$
CC	OC	1.26	439320.0
CC	CT2	1.52	167360.0
CT2	HA	1.11	258571.2
OH1	H	0.96	456056.0
CT	CC	1.52	167360.0
CT2	CT	1.50	186188.0
CT	OH1	1.42	358150.4

Table E2: Bonded parameters for V^{bond} , taken from existing parameters in the CHARMM FF.

			$\theta_0 / ^\circ$	$k_\theta / \text{kJ mol}^{-1}$	$r_{UB} / \text{\AA}$	$k_{UB} / \text{kJ mol}^{-1}$
OC	CC	OC	124.00	836.80	2.225	58576.000
OC	CC	CT2	118.00	334.72	2.388	41840.000
CC	CT2	HA	109.50	276.14	2.163	25104.000
HA	CT2	HA	109.00	297.06	1.802	4518.720
CT	CC	OC	118.00	334.72	2.388	41840.000
CT2	CT	CC	108.00	435.14	0.000	0.000
CT2	CT	CT2	113.60	488.27	2.561	9338.688
HA	CT2	CT	110.10	279.74	2.179	18853.104
CC	CT2	CT	108.00	435.14	0.000	0.000
CT2	CT	OH1	110.10	633.46	0.000	0.000
OH1	CT	CC	110.10	633.46	0.000	0.000
CT	OH1	H	106.00	481.16	0.000	0.000

Table E3: Bonded parameters for V^{angle} , taken from existing parameters in the CHARMM FF.

				$\phi_0/^\circ$	$k_\phi/\text{kJ mol}^{-1}$	n
HA	CT2	CC	OC	180.00	0.2092	6
CT	CT2	CC	OC	180.00	0.2092	6
<u>CT2</u>	<u>CT</u>	<u>CT2</u>	<u>CC</u>	0.00	4.0000	3
OH1	CT	CT2	CC	0.00	0.8368	3
OH1	CT	CT2	HA	0.00	0.8368	3
CC	CT	CT2	CC	0.00	0.8368	3
CC	CT	CT2	HA	0.00	0.8368	3
CT2	CT	CT2	HA	0.00	0.8368	3
<u>OH1</u>	<u>CT</u>	<u>CC</u>	<u>OC</u>	0.00	1.2000	2
CT2	CT	CC	OC	180.00	0.2092	6
<u>CC</u>	<u>CT</u>	<u>OH1</u>	<u>H</u>	0.00	0.2092	1
CT2	CT	OH1	H	0.00	0.5858	3

Table E4: Bonded parameters for $V^{dihedral}$, taken from existing parameters in the CHARMM FF. Parameters for torsional terms refined specifically in this work have been underlined.

				$\eta_0/^\circ$	$k_\eta^{CHARMM}/\text{kJ mol}^{-1}$
CC	CT2	OC	OC	0.000	803.328
CC	CT	OC	OC	0.000	803.328

Table E5: Bonded parameters for $V^{improper}$, taken from existing parameters in the CHARMM FF.

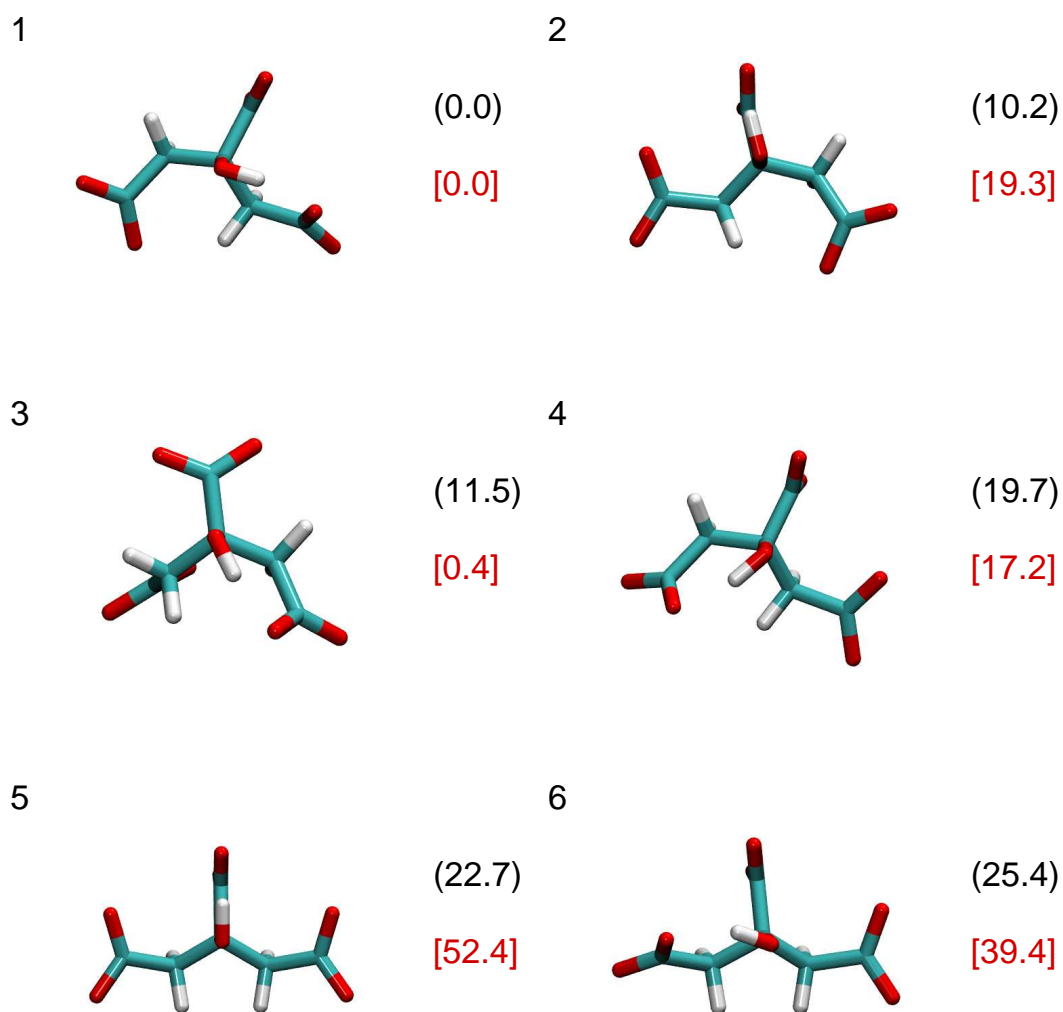


Figure E5: Optimal geometry of the citrate anion *in vacuo* in a number of different internal configurations identified by calculations at the MP2/6-31G* level. The energy (kJmol^{-1}) of each structure relative to the ground state is given. Data in black with round brackets were obtained using MP2/6-31G* calculations, whilst those shown in red with square brackets were generated using the FF. The MP2 data were not used in our fitting procedure.

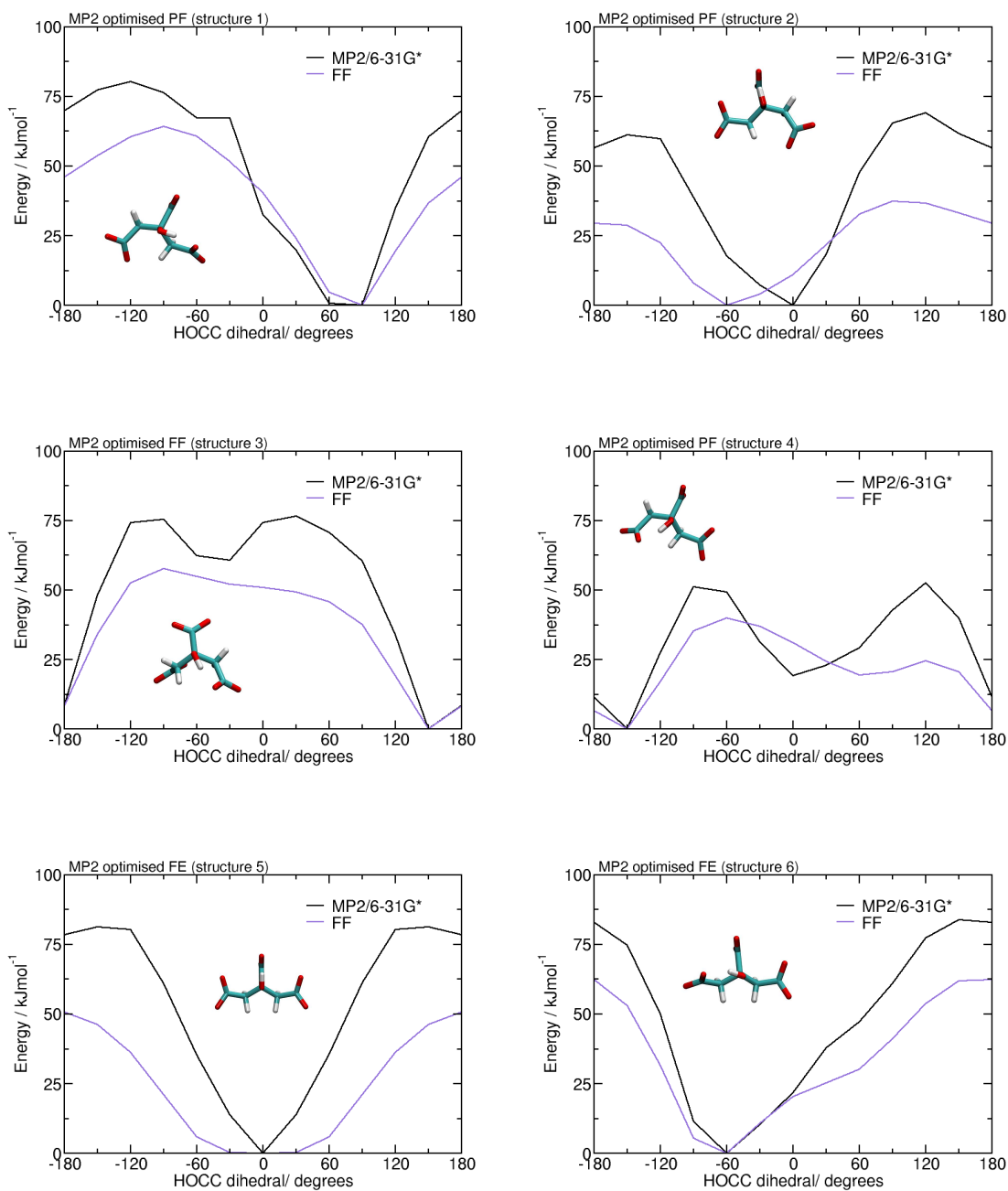


Figure E6: Potential energy scans of HOCC dihedral for each of the optimised structures of citrate *in vacuo* shown in Figure E5. Data are presented for calculations carried out at the MP2/6-31G* level (not used in our fitting procedure) and using the new FF parameters.

run		Average number	Average length/Å
CPMD A	total COO ⁻ ··· water	11.586±1.257	1.883±0.223
CPMD A	internal	0	n/a
CPMD A	OH··· water	1.002±0.621	2.060±0.198
CPMD A	HO··· water	0.801±0.399	1.997±0.212
FF-s A	total COO ⁻ ··· water	18.437±1.393	1.801±0.206
FF-s A	internal	0.001±0.035	1.734±0.016
FF-s A	OH··· water	1.061±0.657	2.061±0.176
FF-s A	HO··· water	0.341±0.474	2.103±0.238
CPMD B	total COO ⁻ ··· water	11.245±1.153	1.849±0.194
CPMD B	internal	0.817±0.387	1.819±0.159
CPMD B	OH··· water	0.670±0.497	2.009±0.177
CPMD B	HO··· water	0.061±0.239	2.281±0.093
FF-s B	total COO ⁻ ··· water	15.744±1.800	1.853±0.193
FF-s B	internal	0.551±0.497	1.997±0.158
FF-s B	OH··· water	0.788±0.409	2.021±0.176
FF-s B	HO··· water	0.146±0.353	2.234±0.138
FF-s C	total COO ⁻ ··· water	18.639±1.365	1.836±0.185
FF-s C	internal	0.753±0.431	1.882±0.131
FF-s C	OH··· water	1.607±0.661	2.018±0.173
FF-s C	HO··· water	0.036±0.186	2.256±0.124

Table E6: Average number and average length of citrate··· water hydrogen-bonds found in CPMD and FF-s simulations initiated in configurations A, B and C.

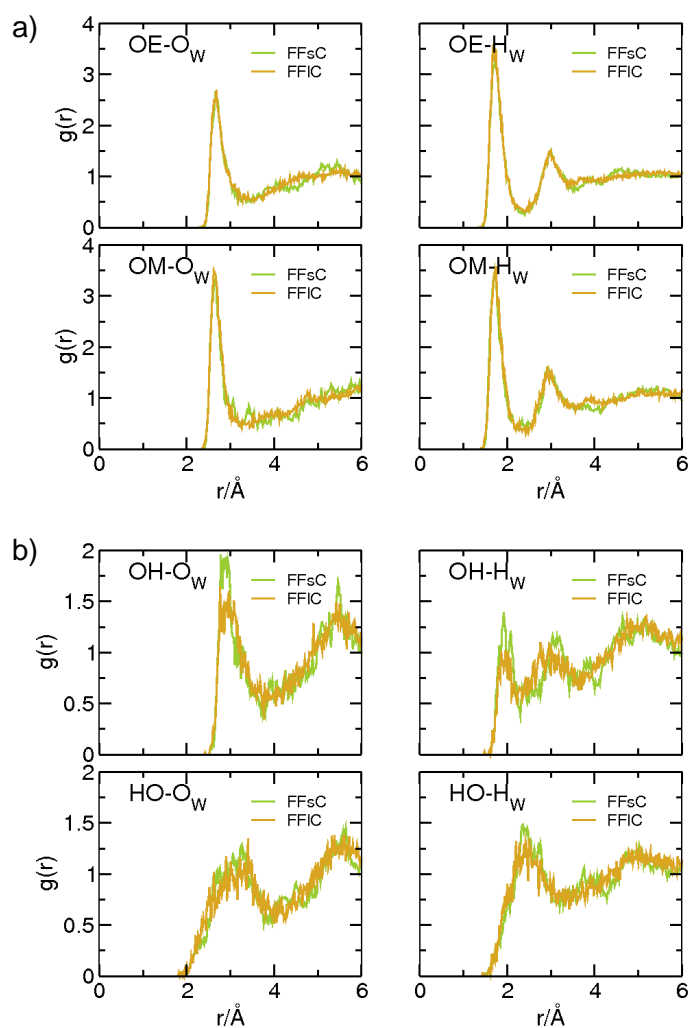


Figure E7: RDF profiles for citrate a) carboxylate⁻ and b) hydroxyl⁻ O_w and H_w distances for FF-s and FF-l simulations initiated in the C conformation.

Hydrogen-Bond Strength

The characteristic lifetime of a hydrogen-bond is one way of estimating its strength. Two alternative methods have been proposed in the literature. The first (denoted ‘Method 1’ below) is based on the ratio between the heights of the first peak and trough in the Radial Distribution (RDF) profiles of the two interacting species,¹ whilst the second (denoted ‘Method 2’ below) is based on the average length of a hydrogen-bond.²

Method 1

Furmanchuk *et al.* estimated the strength of a hydrogen-bond between water and nucleic acid bases adenine, thymine, guanine and cytosine by taking the ratio g^{max}/g^{min} from the relevant RDF profiles of the molecules simulated in liquid water using CPMD.¹ In this work, g^{max} has been chosen using the condition that $r^{max} < 2.45 \text{ \AA}$; the same distance used as a cut-off for H \cdots O interactions for the rigorous description of a hydrogen-bond outlined in the ‘Methods’ section. Figure E8 shows the results of applying this method to estimate hydrogen-bond strength to CPMD, FF-s and FF-l simulations of citrate.

Whilst using the method of Furmanchuk *et al.* to determine hydrogen-bond strength¹ there were no significant differences between CPMD and FF data for carboxylate \cdots water hydrogen-bonds, the same was not true for hydroxyl \cdots water ones; the strength of the latter were consistently underestimated by the FF. However, in agreement with CPMD, both FF-s and FF-l showed a slight tendency for OE carboxylate \cdots water hydrogen-bonds to be stronger than OM ones. This also concurred with the trend observed when characteristic lifetime was used as the metric of hydrogen-bond strength.

It is important to note that this method of defining hydrogen-bond strength is based on a single distance criterion only. As mentioned in the ‘Results and Discussion’ Section this does not preclude two molecules which may merely be in close proximity, but not actually hydrogen-bonded to each other. The former scenario is likely to account for the exceedingly strong hydrogen-bond between O(-H) and water in CPMD B, where water molecules residing the first hydration shell of the hydroxyl O may be attracted to this location not only by the O

itself but also by the Na⁺ co-ordinated to it.

Method 2

Lee *et al.* optimized the structure of a number of cationic, neutral and anionic N/O...H hydrogen-bonded dimers *in vacuo* using the BLYP and B3LYP functionals and at the MP2 level of theory.² They found that the binding energy was proportional to $1/r^4$, where r was the length of the hydrogen-bond between the two monomers. Whilst these calculations were carried out under different conditions to those used in the CPMD and FF MD simulations of citrate presented here (*i.e. in vacuo vs. aqueous*, and at 0 K rather than 300 K), it was interesting to investigate whether trends in citrate-water hydrogen-bond strength predicted by this method were in agreement with the other two metrics (Method 1 above, and hydrogen-bond lifetime) used.

Again, in agreement with Method 1 and the hydrogen-bond lifetime metric of hydrogen-bond strength, citrate...water hydrogen-bonds formed in CPMD simulations were of comparable strength to those formed in FF-s and FF-l simulations (Figure E9) when using this metric. In all simulations carboxylate...water hydrogen-bonds are stronger than hydroxyl...water ones.

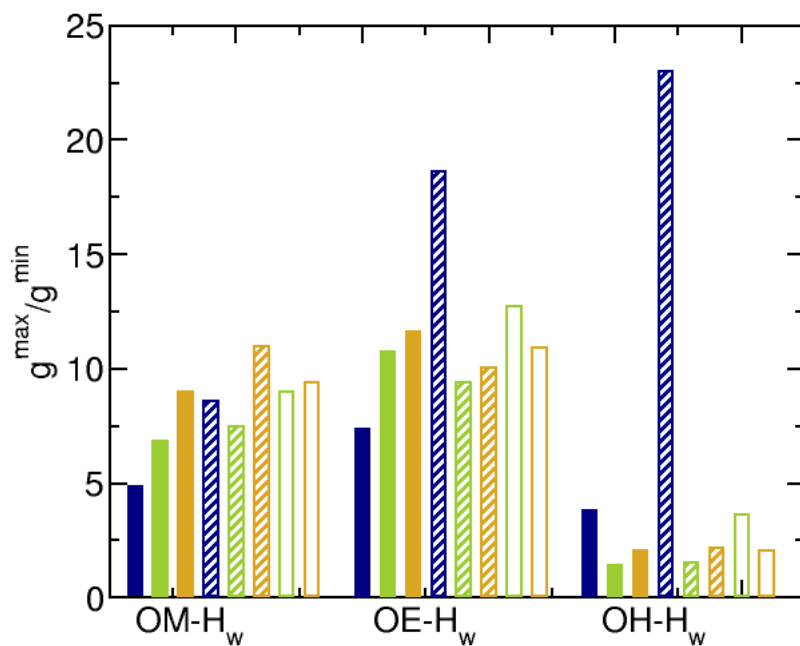


Figure E8: Hydrogen-bond strength (defined by the ratio g^{max}/g^{min}) for OM-water, OE-water and OH-water hydrogen-bonds for CPMD (navy), FF-s (green) and FF-l (yellow) simulations initiated in starting conformations A (solid fill), B (patterned fill) and C (unfilled).

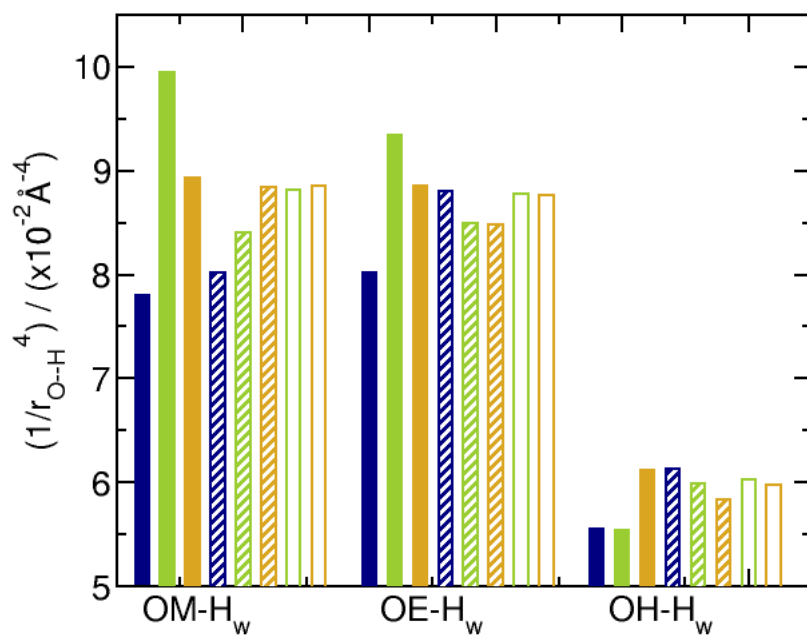


Figure E9: Hydrogen-bond strength (defined as being proportional to $1/r_{O-H}^4$) for OM-water, OE-water and OH-water hydrogen-bonds for CPMD (navy), FF-s (green) and FF-l (yellow) simulations initiated in starting conformations A (solid lines), B (dashed lines) and C (dotted lines).

		τ_S^{CPMD}/ps	τ_S^{FF-s}/ps
A	OM	0.2	0.4
A	OE	0.7	0.5
A	OH	0.1	0.2
A	HO	0.4	0.1
B	OM	0.4	0.7
B	OE	1.4	0.6
B	int	0.1	0.0
B	OH	0.4	0.4
B	HO	0.0	0.0
C	int	n/a	0.1

Table E7: Continuous hydrogen-bond lifetimes, τ_S , for $\text{COO}^- \cdots$ -water (OM and OE), $\text{OH} \cdots$ -water, $\text{HO} \cdots$ -water, and, internal hydrogen-bonds for CPMD and FF-s simulations starting in conformations A and B. Continuous hydrogen-bond lifetime for the internal hydrogen-bond in simulation FF-s C is also shown.

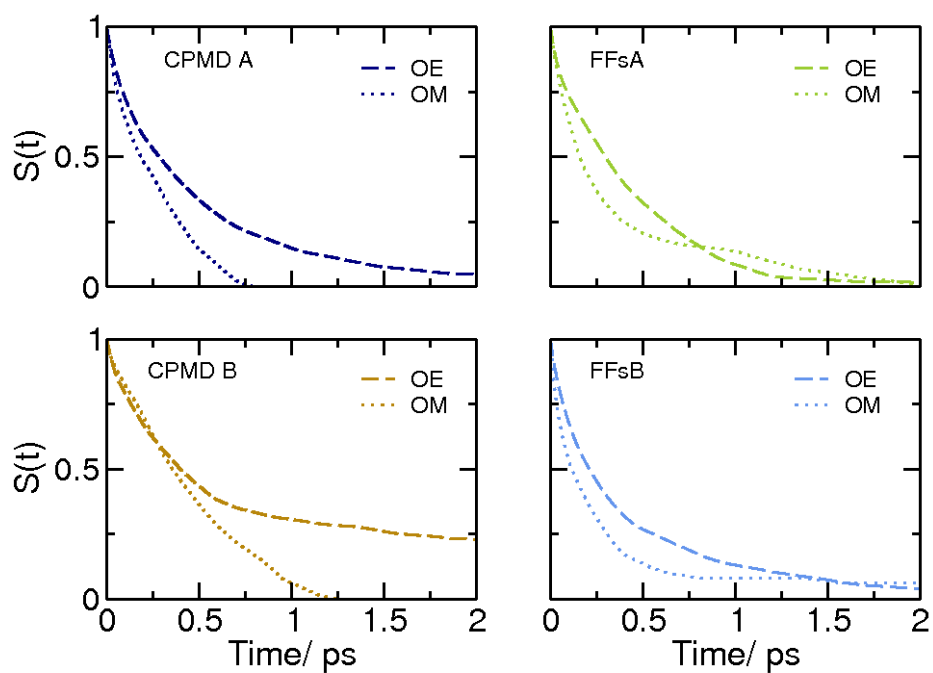


Figure E10: Continuous hydrogen-bond time-autocorrelation functions, $S(t)$, for carboxylate...water hydrogen-bonds formed by citrate for CPMD and FF-s simulations starting in conformations A and B. Hydrogen-bonds formed by OE O are shown as dashed lines, whilst those formed by OM O are shown as dotted.

Amino Acid Simulation Methods

To investigate the persistence of carboxylate...water hydrogen-bonds modelled by CHARMM FF, four simulations of glycine under aqueous conditions were carried out. Two protonation states of glycine have been modelled—the zwitterionic form of the amino acid, stable in solution at pH 7, and the anionic form, stable under basic conditions—to investigate the influence of overall charge density on the structuring of water molecules surrounding the molecule. In both cases two sets of simulations were performed, either identical to the FF-s or FF-l citrate runs (see Section ‘Methods: Force-field MD Simulations’). The zwitterionic glycine simulations comprised 1 glycine and 494 TIP3P water molecules, whilst the anionic glycine simulations comprised 1 glycine, 1 Na⁺ and 1276 TIP3P water molecules.

Similarly, to probe the CHARMM description of an hydroxyl...water hydrogen-bond, simulations of serine and threonine under aqueous conditions were carried out. As before, conditions identical to those in citrate runs FF-s were employed. The serine simulation comprised 1 serine and 500 TIP3P water molecules, whilst the threonine simulation comprised 1 threonine and 470 TIP3P water molecules.

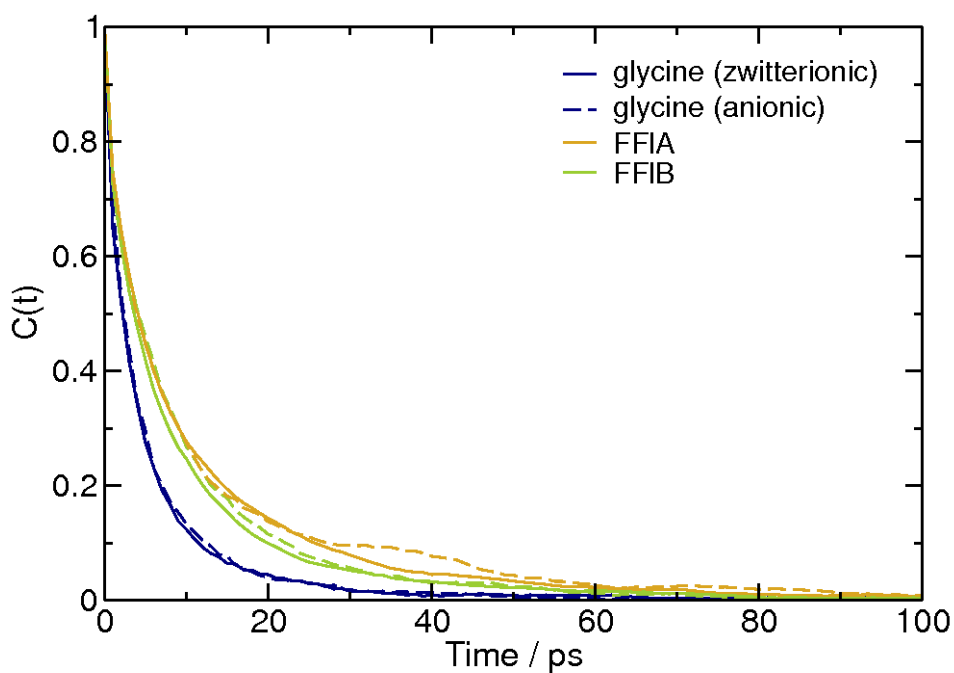


Figure E11: Intermittent hydrogen-bond time-autocorrelation functions, $C(t)$, for carboxylate...water hydrogen-bonds formed by citrate for FF-I simulations starting in conformations A (yellow) and B (green). Hydrogen-bonds formed by OE oxygen atoms are shown as solid lines, whilst those formed by OM oxygen atoms are shown as dashed. Carboxylate...water hydrogen-bonds formed by glycine (navy) in its zwitterionic (solid line) and anionic (dashed line) forms are also shown for reference.

	H	F	P	E
A	20.2	0.0	47.0	53.0
B	17.6	0.0	20.2	79.8
C	27.0	0.0	19.6	80.4
total	22.3	0.0	19.9	80.1

Table E8: Percentage probability of a structure being internally hydrogen-bonded, calculated over all the possible backbone and Na⁺ co-ordination states (column label 'H'). Percentage probability of a structure having a folded (column 'F'), partially-folded (column 'P') or extended (column 'E') structure, calculated over all possible hydrogen-bonded and Na⁺ co-ordination states. 'Total' is the average of the two sets of simulations initiated in conformations B and C only.

	F	P	E
B	0.0	23.2	16.2
C	0.0	27.9	26.8
total	0.0	25.5	21.5

Table E9: Percentage probability of a structure being internally hydrogen-bonded given it is in a folded (F), partially folded (P) or extended (E) carbon backbone conformation. Data presented only for the 14 simulations started in either initial configuration B or C only. ‘Total’ is the average of the two.

<i>n</i>	0	1	2	3
B	11.6	43.2	35.2	10.0
C	17.5	45.6	35.3	1.6
total	15.2	44.6	35.2	4.9

Table E10: Percentage probability of citrate, when featuring an internal hydrogen-bond, to be co-ordinated by n Na⁺ ions. Data presented only for the 14 simulations started in either initial conformation B or C only. ‘Total’ is the average of the two.

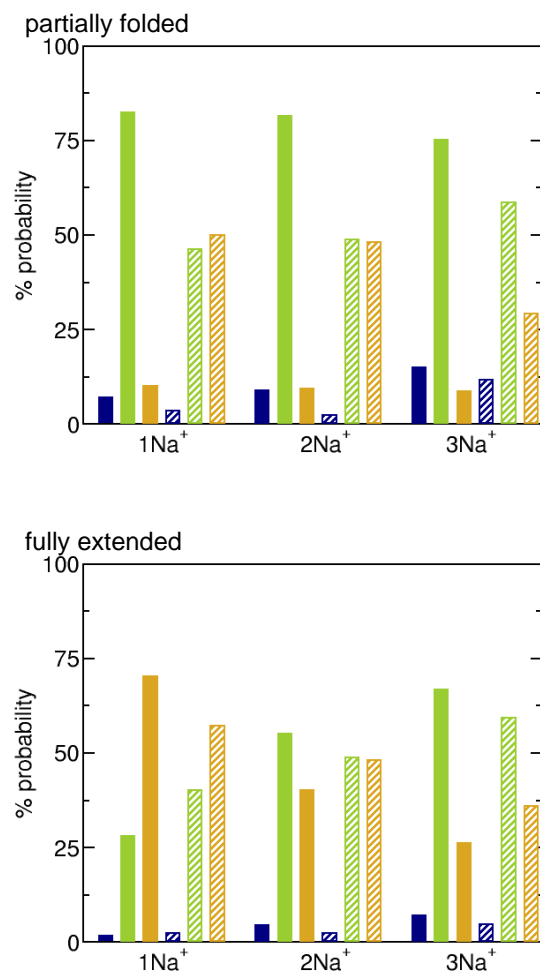


Figure E12: Percentage probability of an Na^+ ion being co-ordinated to 1 (navy), 2 (green) or 3 (yellow) oxygen atoms in citrate for each type of citrate- Na_n^+ ion pair. Partially folded (top) and fully extended citrate structures (bottom) have been sub-categorized into internally hydrogen-bonded (solid fill) and non-internally hydrogen-bonded (patterned fill) conformations. Data was pooled from the 14 simulations initiated in either conformation B or C only.

cluster	config ₁	<i>m</i> ₁	config ₂	<i>m</i> ₂	config ₃	<i>m</i> ₃
p h 1	OM-OE (73.3)	2	OE-OM-OM (7.8)	3	OM (3.9)	1
p n 1	OE-OM-OH (40.9)	3	OM-OE (40.3)	2	OE-OE-OM (7.2)	3
e h 1	OE-OM-OH (69.8)	3	OM-OE (25.2)	2	OH-OE (1.0)	2
e n 1	OE-OM-OH (56.7)	3	OM-OE (37.0)	2	OE (1.3)	1
p h 2	OM-OE (69.2)	2	OE-OM-OM (5.8)	3	OE (5.2)	1
p n 2	OM-OE (44.5)	2	OE-OM-OH (33.0)	3	OE-OE-OM (13.7)	3
e h 2	OM-OE (47.3)	2	OE-OM-OH (38.3)	3	OM-OM (5.5)	2
e n 2	OE-OM-OH (47.7)	3	OM-OE (45.2)	2	OM-OM (1.8)	2
p h 3	OM-OE (54.8)	2	OH-OM (18.3)	2	OM (11.8)	1
p n 3	OM-OE (36.3)	2	OE-OM-OH (19.1)	3	OM-OM (11.7)	2
e h 3	OM-OE (56.2)	2	OE-OM-OH (24.5)	3	OM-OM (6.4)	2
e n 3	OM-OE (52.1)	2	OE-OM-OH (35.5)	3	OM-OM (3.2)	2

Table E11: The three most populated co-ordination states of Na⁺ ions surrounding citrate, config₁, config₂ and config₃. Config_{*x*} labels correspond to the oxygen type—see text for details—to which the Na⁺ ion is co-ordinated. The percentage probability of this configuration occurring for each citrate cluster (denoted p/e, h/n, 1/2/3) is given in parentheses (see text for details of structural classifications assigned to citrate clusters). *m_x* is the number of O atoms to which an Na⁺ ion is co-ordinated in config_{*x*}.

Citrate Input Files:

Below we give the citrate structure file, citrate.gro:

example citrate gro file

18

```
1CIT  CAC  1 -0.271 -0.024  0.008
1CIT  CA   2 -0.131 -0.066 -0.047
1CIT  CB   3  0.000  0.000  0.000
1CIT  CBC  4  0.022  0.143 -0.063
1CIT  CG   5  0.118 -0.090 -0.048
1CIT  CGC  6  0.261 -0.072  0.013
1CIT  OA1  7 -0.299  0.099  0.018
1CIT  OA2  8 -0.351 -0.122  0.030
1CIT  OB1  9  0.053  0.238  0.014
1CIT  OB2 10  0.012  0.146 -0.191
1CIT  OG1 11  0.273 -0.015  0.126
1CIT  OG2 12  0.355 -0.126 -0.054
1CIT  OHB 13 -0.000  0.000  0.144
1CIT  HA1 14 -0.124 -0.174 -0.029
1CIT  HA2 15 -0.133 -0.051 -0.156
1CIT  HG1 16  0.091 -0.195 -0.027
1CIT  HG2 17  0.126 -0.080 -0.157
1CIT  HOB 18  0.096 -0.014  0.162
3.00000  3.00000  3.00000
```

The topology file, citrate.top, is given below:

[defaults]

1 2 yes 1.0 1.0

[atomtypes]

OC	8	15.9999	-0.760	A	0.302906	0.50208
CC	6	12.0110	0.620	A	0.356359	0.29288
HA	1	1.0080	0.090	A	0.235197	0.09205
CT2	6	12.0110	-0.180	A	0.387541	0.23012
CT	6	12.0110	-0.070	A	0.405359	0.08368
OH1	8	15.9999	-0.540	A	0.315378	0.63639
H	1	1.0080	0.310	A	0.040001	0.19623

[bondtypes]

CC	OC	1	0.126	439320.0
CC	CT2	1	0.152	167360.0
CT2	HA	1	0.111	258571.2
OH1	H	1	0.096	456056.0
CT	CC	1	0.152	167360.0
CT2	CT	1	0.150	186188.0
CT	OH1	1	0.142	358150.4

[angletypes]

OC	CC	OC	5	124.00	836.80	0.2225	58576.000
OC	CC	CT2	5	118.00	334.72	0.2388	41840.000
CC	CT2	HA	5	109.50	276.14	0.2163	25104.000
HA	CT2	HA	5	109.00	297.06	0.1802	4518.720
CT	CC	OC	5	118.00	334.72	0.2388	41840.000
CT2	CT	CC	5	108.00	435.14	0.0000	0.000
CT2	CT	CT2	5	113.60	488.27	0.2561	9338.688
HA	CT2	CT	5	110.10	279.74	0.2179	18853.104
CC	CT2	CT	5	108.00	435.14	0.0000	0.000
CT2	CT	OH1	5	110.10	633.46	0.0000	0.000
OH1	CT	CC	5	110.10	633.46	0.0000	0.000
CT	OH1	H	5	106.00	481.16	0.0000	0.000

[dihedraltypes]

HA	CT2	CC	OC	9	180.00	0.2092	6
CT	CT2	CC	OC	9	180.00	0.2092	6
CT2	CT	CT2	CC	9	0.00	4.0000	3
OH1	CT	CT2	CC	9	0.00	0.8368	3
OH1	CT	CT2	HA	9	0.00	0.8368	3
CC	CT	CT2	CC	9	0.00	0.8368	3
CC	CT	CT2	HA	9	0.00	0.8368	3
CT2	CT	CT2	HA	9	0.00	0.8368	3
OH1	CT	CC	OC	9	0.00	1.2000	2
CT2	CT	CC	OC	9	180.00	0.2092	6

CC	CT	OH1	H	9	0.00	0.2092	1
CT2	CT	OH1	H	9	0.00	0.5858	3
CC	CT2	OC	OC	2	0.00	803.328	
CC	CT	OC	OC	2	0.00	803.328	

[moleculetype]

CIT 3

[atoms]

1	CC	1	CIT	CAC	1	0.620	12.011
2	CT2	1	CIT	CA	2	-0.180	12.011
3	CT	1	CIT	CB	3	-0.070	12.011
4	CC	1	CIT	CBC	4	0.620	12.011
5	CT2	1	CIT	CG	5	-0.180	12.011
6	CC	1	CIT	CGC	6	0.620	12.011
7	OC	1	CIT	OA1	7	-0.760	15.999
8	OC	1	CIT	OA2	8	-0.760	15.999
9	OC	1	CIT	OB1	9	-0.760	15.999
10	OC	1	CIT	OB2	10	-0.760	15.999
11	OC	1	CIT	OG1	11	-0.760	15.999
12	OC	1	CIT	OG2	12	-0.760	15.999
13	OH1	1	CIT	OHB	13	-0.540	15.999
14	HA	1	CIT	HA1	14	0.090	1.008
15	HA	1	CIT	HA2	15	0.090	1.008
16	HA	1	CIT	HG1	16	0.090	1.008
17	HA	1	CIT	HG2	17	0.090	1.008
18	H	1	CIT	HOB	18	0.310	1.008

[bonds]

1	8	1
1	7	1
1	2	1
2	15	1
2	14	1
2	3	1
3	13	1
3	5	1
3	4	1
4	10	1
4	9	1
5	17	1
5	16	1
5	6	1
6	12	1
6	11	1
13	18	1

[angles]

8	1	7	5
8	1	2	5

7	1	2	5
1	2	15	5
15	2	14	5
15	2	3	5
1	2	14	5
14	2	3	5
1	2	3	5
2	3	13	5
13	3	5	5
13	3	4	5
2	3	5	5
5	3	4	5
2	3	4	5
3	4	10	5
10	4	9	5
3	4	9	5
3	5	17	5
17	5	16	5
17	5	6	5
3	5	16	5
16	5	6	5
3	5	6	5
5	6	12	5
12	6	11	5
5	6	11	5
3	13	18	5

[exclusions]

18 9 10

[pairs]

10 18 2 0.3 -0.760 0.310 0.17145 0.310857

9 18 2 0.3 -0.760 0.310 0.17145 0.310857

[dihedrals]

8	1	2	15	9
7	1	2	15	9
8	1	2	14	9
7	1	2	14	9
8	1	2	3	9
7	1	2	3	9
1	2	3	13	9
15	2	3	13	9
14	2	3	13	9
1	2	3	5	9
15	2	3	5	9
14	2	3	5	9
1	2	3	4	9
15	2	3	4	9
14	2	3	4	9
2	3	13	18	9

5	3	13	18	9
4	3	13	18	9
2	3	5	17	9
13	3	5	17	9
4	3	5	17	9
2	3	5	16	9
13	3	5	16	9
4	3	5	16	9
2	3	5	6	9
13	3	5	6	9
4	3	5	6	9
2	3	4	10	9
13	3	4	10	9
5	3	4	10	9
2	3	4	9	9
13	3	4	9	9
5	3	4	9	9
3	5	6	12	9
17	5	6	12	9
16	5	6	12	9
3	5	6	11	9
17	5	6	11	9
16	5	6	11	9

[dihedrals]

1	2	7	8	2
4	3	9	10	2
6	5	11	12	2

[system]

citrate

[molecules]

CIT 1

References

- [1] A. Furmanchuk, O. Isayev, O. V. Shishkin, L. Gorb, and J. Leszczynski, *Phys. Chem. Phys. Chem.*, 2010, **12**, 3363.
- [2] K. Lee, E. D. Murray, L. Kong, B. I. Lundqvist, and D. C. Langreth, *Phys. Rev. B*, 2010, **82**, 081101.
- [3] X. Qian and X. Wei, *J. Phys. Chem. B*, 2012, **116**(35), 10898.
- [4] M. Galib and G. Hanna, *J. Phys. Chem. B*, 2011, **115**, 15024.
- [5] J. Stare, J. Mavri, J. Grdadolnik, J. Zidar, Z. B. Maksic, and R. Vianello, *J. Phys. Chem. B*, 2011, **115**, 5999.
- [6] M. P. Allen and D. J. Tildesley, *Computer Simulation of Liquids*, Oxford University Press, Oxford, 1987.